



Trade Science Inc.

ISSN : 0974 - 7486

Volume 7 Issue 3

Materials Science

An Indian Journal

Full Paper

MSAIJ, 7(3), 2011 [152-160]

Some magnetic properties of Cu-Ge ferrite in low magnetic field

S.A.Mazen*, N.I.Abu-Elsaad

Magnetic and Semiconductor Laboratory, Physics Department, Faculty of Science, Zagazig University, Zagazig, (EGYPT)

E-mail : dr.saidmazen@gmail.com

Received: 15th November, 2010 ; Accepted: 25th November, 2010

ABSTRACT

Some magnetic properties such as B-H loops and initial permeability μ_i for the polycrystalline soft ferrite, $Cu_{1-x}Ge_xFe_{2-2x}O_4$; with $x=0.0, 0.05, 0.1, 0.15, 0.2, 0.25$ and 0.3 have been studied. The B-H loops were first measured at RT as a function of magnetizing current I from 0.5 to $6A$ (i.e. $H=185Am^{-1}$ to $3250Am^{-1}$). It was found that the coercive force H_c increases with increasing the magnetizing current but the relative magnetization m_r shows a maximum value for each composition at I between $2-3A$. Also, The B-H loops were measured at elevated temperature and constant magnetizing current ($I=2.5A$ which is equivalent to $900Am^{-1}$). It was observed that H_c decreases with increasing the temperature. The initial permeability μ_i was measured as a function of temperature for the above investigated ferrite. Utilizing the initial permeability data, the Curie temperature T_c and the paramagnetic temperature T_p were estimated. These values of temperature (T_c & T_p) have been found to decrease with increasing Ge^{4+} ions content.

© 2011 Trade Science Inc. - INDIA

KEYWORDS

Ferrite;
Magnetization;
B-H loop;
Initial permeability.

INTRODUCTION

Ferrites are still much used in permanent magnets market because of their low price combined with reasonable magnetic performances. Another advantage is the great chemical stability of these oxides which makes in such a context a little improvement of their magnetic properties of great importance^[1]. Soft ferrites have been extensively used for many kinds of magnetic devices such as transformers, inductors and magnetic heads for high frequency because their electrical resistivity is higher than those of the soft magnetic alloys. Various substitutions have been incorporated to achieve desired electrical and magnetic properties. Ferrites containing cop-

per have shown interesting electrical and magnetic properties^[2-5]. Several studies have reported addition of divalent, trivalent and tetravalent ions and various parameters have been measured depending on the desired application^[6-9]. Our previous works have studied X-ray analysis, IR absorption and electrical properties of Cu-Ge and Cu-Ti ferrites^[10-12]. Also, the influence of the cation distribution on the mössbour spectra of Cu-Ge ferrite has been studied^[13]. Recently, X-ray diffraction (XRD), scanning electron microscope (SEM) and some magnetic properties such as magnetization and B-H loops were measured in analogous study in low magnetic field between Cu-Ge and Cu-Si ferrites^[14].

In the present work, the influence of iron substitu-

tion by tetravalent Ge^{4+} ion on the magnetic properties of Cu-ferrite will be study.

EXPERIMENTAL TECHNIQUE

The mixed copper – germanium ferrite with the chemical formula $\text{Cu}_{1+x}\text{Ge}_x\text{Fe}_{2-2x}\text{O}_4$ (where, $x = 0.0, 0.05, 0.1, 0.15, 0.2, 0.25$ and 0.3) were prepared by using the standard ceramic technique.

The B - H loops were measured for the toroidal sample where the number of turns of the primary coil N_p and the secondary coils N_s , were 16 and 8, respectively. The results were recorded by the aid of a storage oscilloscope (HAMEG, type HM407) connected with pc. The details of the circuit diagram, measurement technique and the calculations were mentioned in our previous work^[14].

The initial permeability μ_i was measured as a function of temperature at constant frequency $f = 10 \text{ KHz}$ and low magnetizing current $i_p = 20 \text{ mA}$. More details about the measurement techniques and calculations of μ_i were explained in our previous work^[15,16].

RESULTS AND DISCUSSION

Effect of magnetizing current on B-H loops

The hysteresis loops were firstly studied at room temperature at constant frequency ($\approx 50 \text{ Hz}$) for all the above investigated compositions of Cu-Ge ferrite. The measurements were carried out in the range of magnetizing current from 0.5 A to 6 A (i.e., from $H = 185 \text{ Am}^{-1}$ to 2250 Am^{-1}). Figure 1 shows the hysteresis loops for CuFe_2O_4 at $I = 1.5$ and 6 A , as a representative example. From the B - H loops, some parameters such as: coercive field H_c (Am^{-1}), remanence induction B_r (T), saturation induction B_s (T), and the relative magnetization ($m_r = B_r/B_s$) were estimated as a function of magnetizing current (I) for all compositions. Figure 2 & 3 represent the effect of magnetizing current I on the coercive field H_c and the relative magnetization m_r , respectively.

The behaviour of the coercive field H_c versus the magnetizing current I could be divided into two regions I & II, where region I for lower than 3 A and region II for higher than 3 A as shown in figure 2. In region I, the coercive field increases gradually with increasing the magnetizing current. In region II, coercive field H_c has

stabilization with increasing the magnetizing current for composition of x up to 0.2 as shown in figure 2a. But, for $x = 0.25$ & 0.3 , the increment of H_c in region II is less than in region I as presented in figure 2b. The stabilization behaviour of H_c may be related to the samples behave as a single domain.

The effect of the magnetizing current I on the relative magnetization m_r were studied as shown in figure 3. It was observed that m_r shows a peak (max. value) between $I = 2-3 \text{ A}$. So that the ratio m_r vs. I could be divided into two stages (I & II). The increment of m_r in stage I and the decrement in stage II depends on the divergence between B_r & B_s . The highest value of $(m_r)_{\text{max}}$ was recorded for $x = 0.05$ at magnetizing current $I = 2 \text{ A}$. This means that loop at this condition can be used for the recording system.

Also, the effect of porosity on the parameters H_c , B_r and B_s at magnetizing current 2.5 A was studied as shown in Fig. 4a-b. It is observed that H_c is directed to small increasing with increasing porosity. This effect may be caused by the fact that the high-porosity samples contain smaller particles, which have higher coercive forces^[17]. But two magnetic parameters B_r and B_s decrease with increasing porosity as shown in figure 4b. This behaviour may be related to the increase in porosity (i.e. decrease in density) or decreasing of magnetic materials in a specified volume accompanied with the decrease in the two parameters B_s and B_r ^[18].

Effect of temperature

The hysteresis loops

Again, the (B - H) loops of $\text{Cu}_{1+x}\text{Ge}_x\text{Fe}_{2-2x}\text{O}_4$ were studied at elevated temperature (from room temperature up to 750 K) and at constant magnetizing current 2.5 A ($H = 900 \text{ Am}^{-1}$). The recorded loops are shown in Fig. 5; for $x = 0.0$ at $T = 320$ and 670 K . The saturation magnetization M_s (relative to B - H loops) was calculated according to the relation:

$$M_s = \left(\frac{B_s}{\mu_0} - H \right) \quad (1)$$

Figure 6 shows the relation between M_s vs. temperature for $x = 0.0$. It was found that M_s vanishes at a point of temperature (called T_s) closed to Curie point T_c . Below the Curie temperature the presence of non-equivalent sublattices leads to a variety of behaviour of

Full Paper

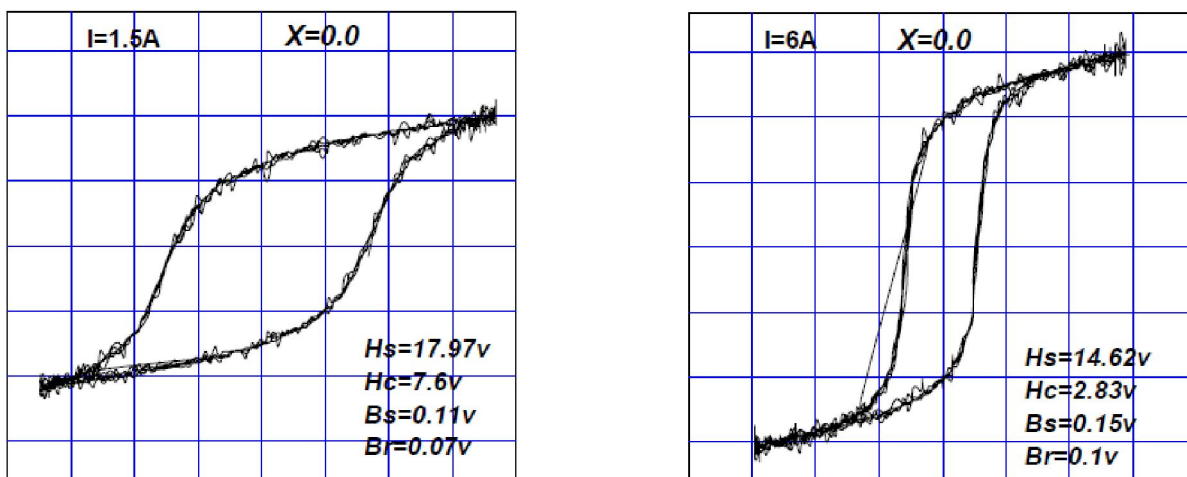


Figure 1 : B-H loops of x=0.0, measured at room temperature (300K) and at I=1.5&6A

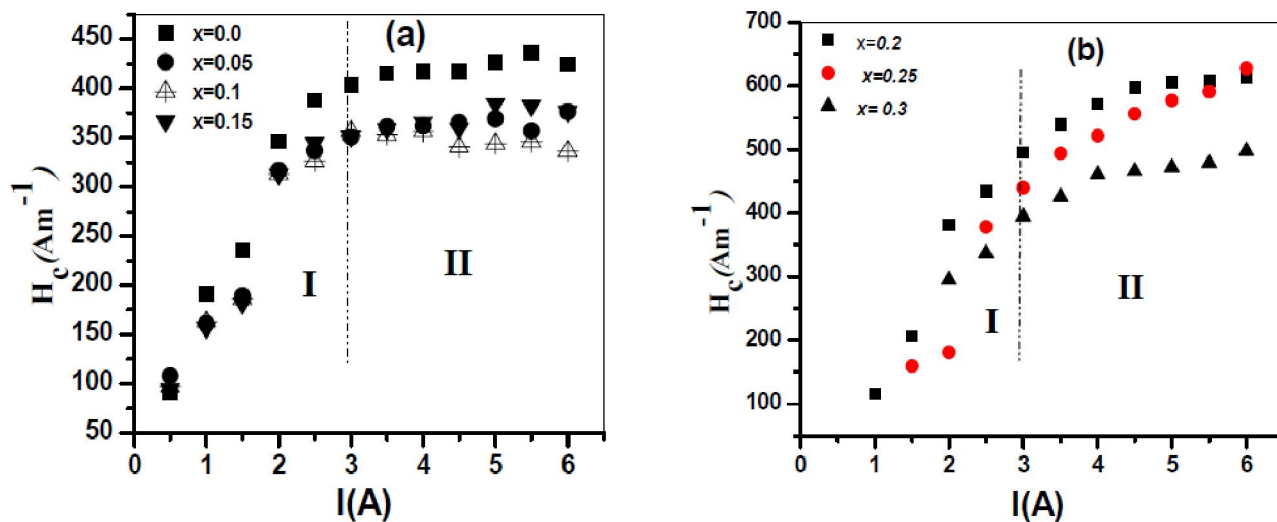


Figure 2 : The effect of magnetizing current on coercive force for $Cu_{1+x}Ge_xFe_{2-2x}O_4$ ($0 \leq x \leq 0.3$)

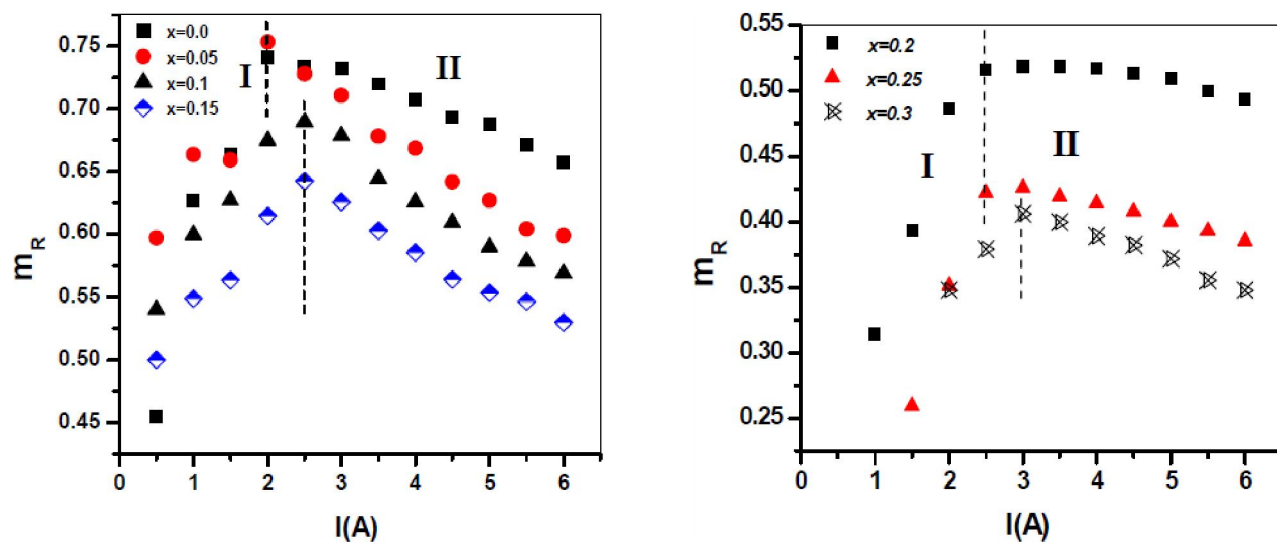


Figure 3 : The effect of magnetizing current on relative magnetization for $Cu_{1+x}Ge_xFe_{2-2x}O_4$ ($0 \leq x \leq 0.3$)

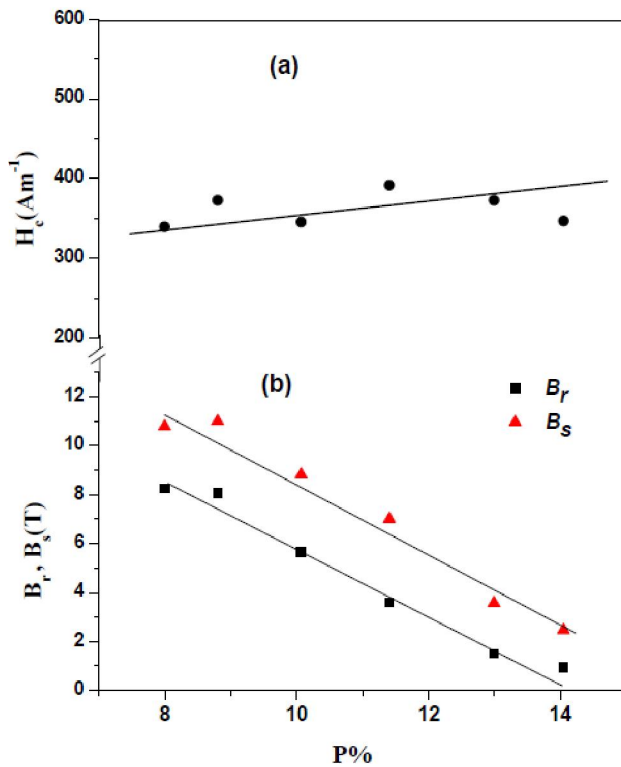


Figure 4a & 4b : The effect of porosity on: a) coercive force and b) remanance and saturation magnetizations

the net magnetization ($M = M_B - M_A$) as a function of temperature, since each sublattice has a magnetic moment with its own temperature dependence. The form of these curves has been explained by Néel in terms of an internal field for each sublattice. The behaviour of M_s vs. T is similar to the behaviour of the magnetization of type R^[18], where one sublattice is not saturated at

OK; a finite value of $\left(\frac{dM}{dT}\right)_H$ is predicted. This may be

shown to conflict the third law of thermodynamics, in which the entropy is independent of the field H when T

$\rightarrow 0$, so $\left(\frac{\delta M}{\delta T}\right)_H \rightarrow 0$. Therefore, $M_s(0)$ can be estimated from the extrapolation curves of figure 6. figure 7 shows the variation of $M_s(0)$ with the addition of Ge content. It observed that it increases up to $x=0.05$ and then decreases with further increases of Ge content. This behaviour can be discussed on the basis of the statistical distribution of the various cations over the A and B-sites using Néel's theorem of two sublattices model^[18]. The individual magnetization, M_A and M_B of the two sublattices cannot be observed, but the calculated magnetic moment for each site μ_A , μ_B and μ_{eff} (i.e.

TABLE 1 : The calculated values of anisotropy constant K , exchange constant A , wall energy σ_w and wall thickness δ_w

X	D (μm)	μ_i	T_c (K)	T_p (K)	K (10^4 J/m ³)	A(0) (10^{-12} J/m)	A(0)	A(T) (10^{-12} J/m)	σ_w (10^{-3} J/m ²)	δ_w (10^{-8} m)
							Theoretically			
0.0	3.97	137.32	718	723	5.13	11.81	12.24	8.98	1.36	2.65
0.05	9.35	195.94	693	716	54.60	11.39	11.81	8.66	4.35	0.79
0.1	23.95	284.78	643	666	44.30	11.6	11.15	7.71	3.70	0.83
0.15	21.24	195.90	613	633	29.30	10.09	10.71	7.18	2.90	0.99
0.2	19.49	131.70	598	623	16.90	9.85	10.45	6.92	2.16	1.28
0.25	16.59	94.01	573	585	1.67	9.44	10.12	6.48	0.66	3.94
0.3	14.93	57.43	553	574	0.92	9.1	9.86	6.12	0.47	5.17

the effective magnetic moment) can be calculated according to:

$$|\vec{\mu}_{eff}| = |\vec{\mu}_B| - |\vec{\mu}_A| \quad (2)$$

The magnetization of each composition depend on the distribution of Fe^{3+} ions among the two sites A and B, where Ge^{4+} ion is non magnetic. On the basis of the above results for the two series, the cation distribution can be suggested as follow^[14]:

$(\text{Cu}_t^{2+} \text{Ge}_x^{4+} \text{Fe}_{1-x-t}^{3+})^A [\text{Cu}_{1+x-t}^{2+} \text{Fe}_{1-x+t}^{3+}]^B \text{O}_4^{2-}$; for $x=0.0$ & 0.05 .

$(\text{Ge}_x^{4+} \text{Fe}_{1-0.6x}^{3+})^A [\text{Cu}_{1+x}^{2+} \text{Fe}_{1-1.4x}^{3+}]^B \text{O}_4^{2-}$; for $(0.1 \leq x \leq 0.3)$.

For the basic ferrite CuFe_2O_4 ($x=0.0$) is known as inverse ferrite, where Cu^{2+} are located on B-sites. However, there is a probability of migration of a small fraction (t) of Cu^{2+} ions to A-sites^[19]; in this case it may be considered as a partially inverse ferrite. For Cu-Ge ferrite, the ionic magnetic moment of Cu^{2+} is 1 and the magnetic moment of Fe^{3+} is 5. The replacement of high spin quantum number ion Fe^{3+} by $x\text{Ge}^{4+}$ ions; where Ge^{4+} ions prefer to occupy A-site^[20], this gives $(1-x-t)\text{Fe}^{3+}$ ions on the A-site and $(1-x+t)\text{Fe}^{3+}$ ions on the B-site. This substitution will lead to increase Fe^{3+} ions on the B-site and consequently the magnetization of the B-site will increase. At the same time the magnetization of the A-site will decrease according to decrease the Fe^{3+} ions on A-site. Accordingly, the net magnetization will increase for $x=0.05$. As the germanium ions increase (in the range of $0.1 \leq x \leq 0.3$), the magnetization decrease with increasing x . This behaviour may be related to the migration of Cu^{2+} ions to B-site. The increase of Ge content will prevent the existence of Cu^{2+} ions on A-site. Also, the

Full Paper

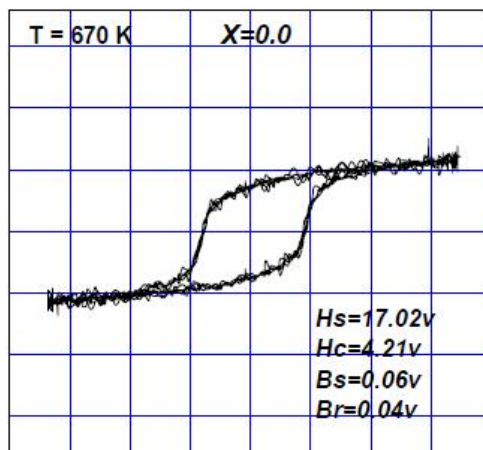
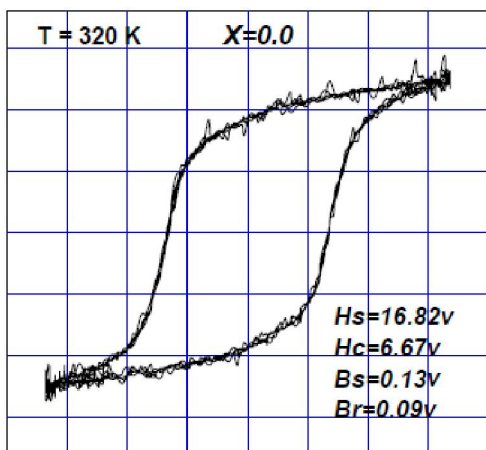


Figure 5 : B-H loops of $x=0.0$, measured at $T=320$ and 670K and constant magnetizing current $I=2.5\text{A}$

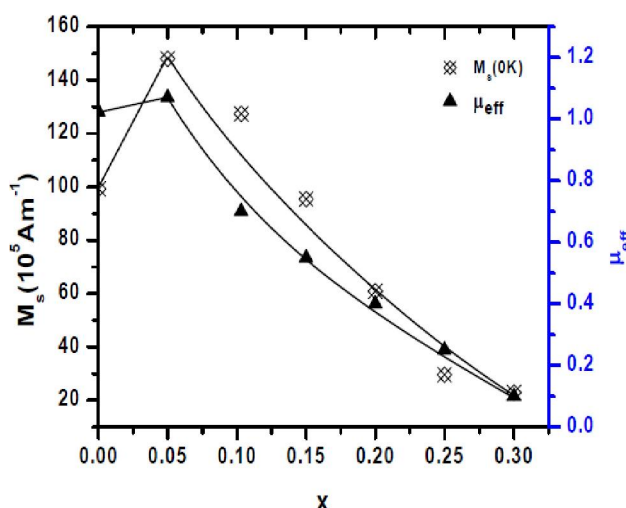
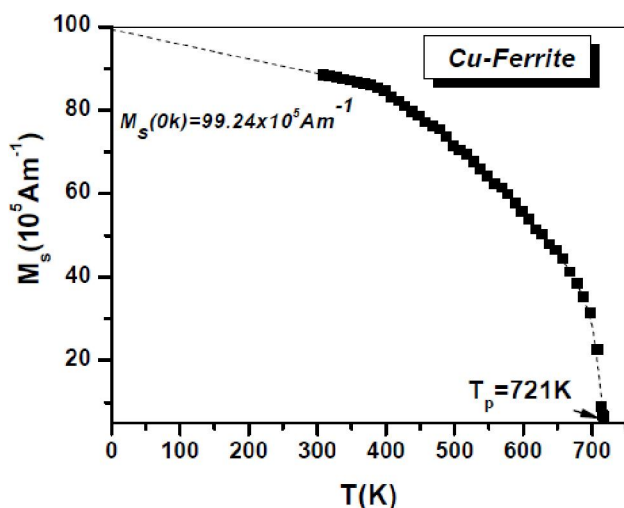


Figure 6 : The effect of temperature on the variation of saturation magnetization for CuFe_2O_4

Figure 7 : The variation of M_s at 0K and the effective magnetic moment μ_{eff} with the composition x

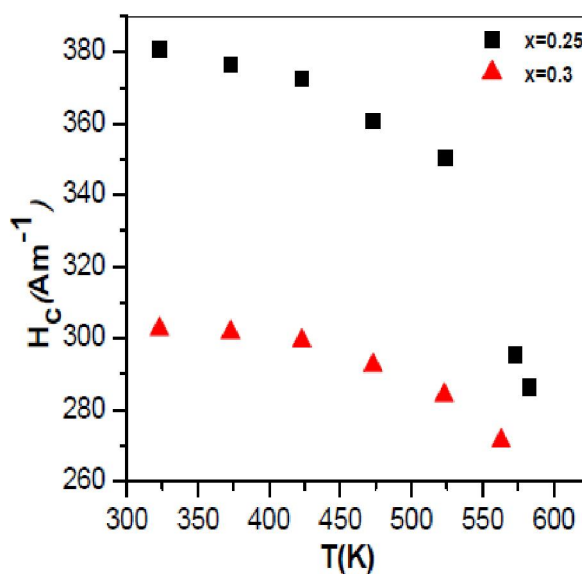
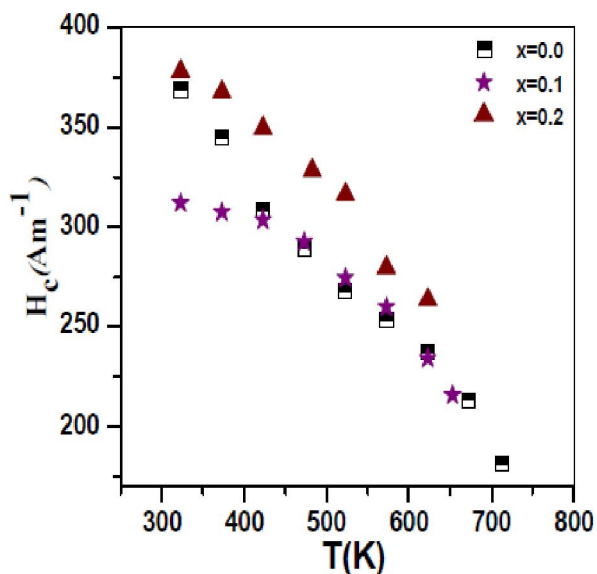


Figure 8 : The effect of temperature on coercive force for $\text{Cu}_{1+x}\text{Ge}_x\text{Fe}_{2-2x}\text{O}_4$ ($0 = x = 0.3$)

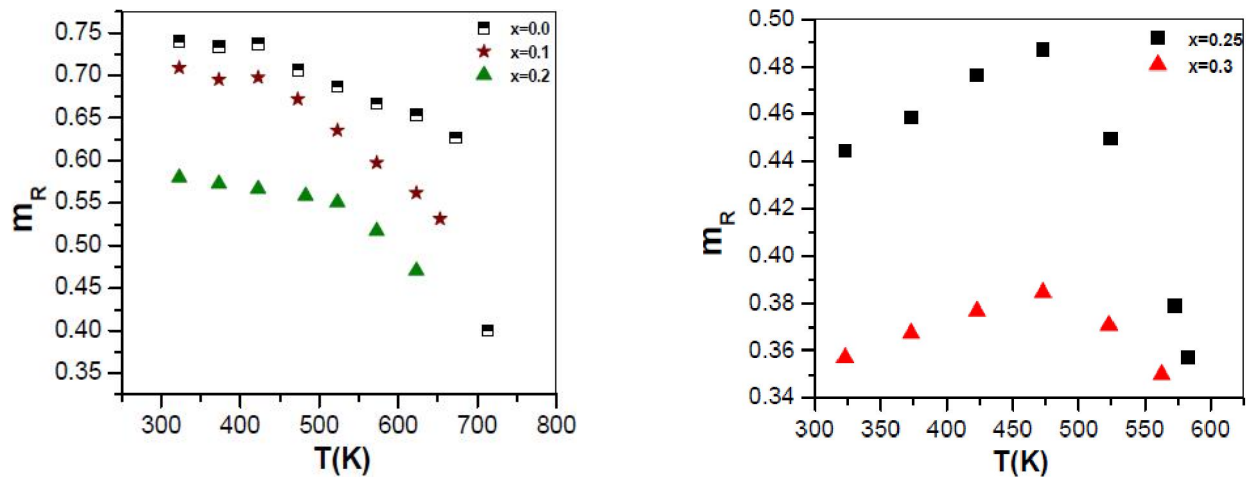


Figure 9 : The effect of magnetizing current on relative magnetization for $\text{Cu}_{1+x}\text{Ge}_x\text{Fe}_{2-2x}\text{O}_4$ ($0 \leq x \leq 0.3$)

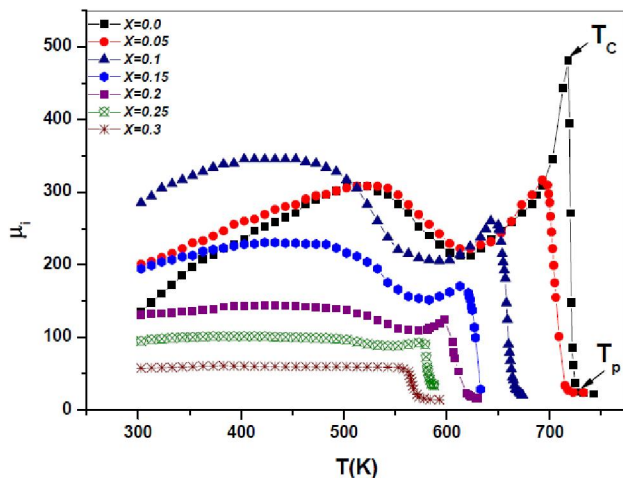


Figure 10 : Thermal spectra of the initial permeability of $\text{Cu}_{1+x}\text{Ge}_x\text{Fe}_{2-2x}\text{O}_4$, ($0.0 \leq x \leq 0.3$)

number of Fe^{3+} ions will decrease on the B-site and increase on A-site. This replacement will weak the magnetization of the whole lattice.

The calculated (effective) magnetic moment μ_{eff} has been determined for Cu-Ge ferrite from the magnetic moment for each site μ_A and μ_B as explained in our previous work^[15] and in the reference of Oxide Magnetic Materials^[18]. It is noticed that the addition of Ge^{4+} ions lead to decrease the magnetic moment in each site (A and B sites). According to Néel's molecular field model, the A-B interaction will be reduced. Therefore, μ_{eff} decreases with increasing the non – magnetic ions of Ge^{4+} in the composition as shown in figure 7. From this figure, μ_{eff} is similar to the behaviour of $M_s(0\text{K})$ versus x . This means the calculation values of μ_{eff} are proportional to the experimental data of saturation magnetization.

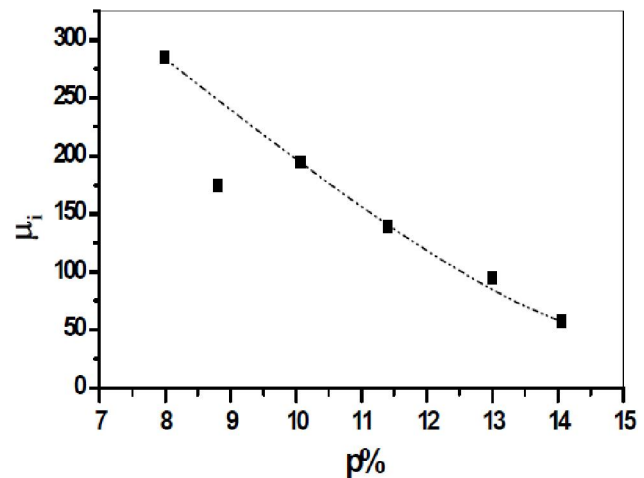


Figure 11 : The variation of initial permeability with percent-age porosity for Cu-Ge ferrite

The variation of coercive field H_c and the relative magnetization m_R with temperature are shown in figure 8 & 9, respectively for all values of x . It can be seen that H_c decreases gradually with increasing the temperature from $x = 0.0$ to 0.2 as shown in figure 8a, but for $x = 0.25$ and 0.3 there is sharp decreasing in H_c for $T \geq 470\text{K}$ (Figure 8b). The relative magnetization m_R decreases with increasing T for $x = 0 \rightarrow 0.2$, but for $x = 0.25$ and 0.3 m_R increases with T for $T \leq 470\text{K}$ and then decreases with further increasing the temperature. This means that m_R shows a maximum value at $T = 470\text{K}$. The behaviour of H_c (and also m_R) could be explained through Brown's relation^[21] which is given by:

$$H_c = \frac{2K_1}{\mu_0 M_s} \quad (3)$$

Full Paper

where K_1 is the anisotropy constant which varies with temperature tending to zero at the transition temperature T_C . It is known that the presence of Fe^{2+} ions in ferrites will affect on the crystal field and consequently on the anisotropy field^[22]. Therefore, the decreasing in K_1 and B_s (i.e M_s) with temperature will reflect on the decreasing behaviour of H_C and $m_R (=B_r/B_s)$.

The initial permeability (μ_i)

The initial permeability μ_i of a ferromagnetic substance can be due either to a simultaneous rotation of the spins in each Weiss domain, or to a reversible displacement or bluging of domain walls. The initial permeability due to rotations is determined by the anisotropies^[17].

The initial permeability μ_i and saturation magnetization M_s are related to the ionic structure and sensitive to the magnetic properties. It is well known that both quantities are complicated functions of temperature.

The thermal spectra of μ_i versus temperature of $Cu_{1-x}Ge_xFe_{2-2x}O_4$ are shown in Fig. 10. It is found that at room temperature, the initial permeability increases till $x=0.1$ and then decreases with further increase of Ge concentration as tabulated in TABLE 1. The sample of $x=0.1$ has the highest value of μ_i while the lowest value of μ_i at $x=0.3$.

It is noticed that μ_i increases with increasing the temperature and falling abruptly close to Curie temperature, T_C . The Curie point T_C "the transition point from ferromagnetic to paramagnetic state" and the paramagnetic point T_p "when the sample becomes completely paramagnetic" were determined from the thermal variation of μ_i vs. T as shown in figure 10. The transition temperature T_C and T_p are tabulated in TABLE 1. It was found that T_p is bit higher than T_C by about 15K. The two temperatures decrease with increasing Ge content. The presence of Ge^{4+} ion in the A-site is weakening the A-B interaction and causes a reduction in the molecular fields (H_m) at the two sites. This leads to a decrease in various magnetic linkages, which mainly reduces H_m and the net result is a decrease in magnetization and consequently a decrease in the Curie temperature.

From the curves of initial permeability versus temperature, (Figure 10), it can be seen that, the specimens of $x = 0.0$ up to 0.15 show a secondary peak

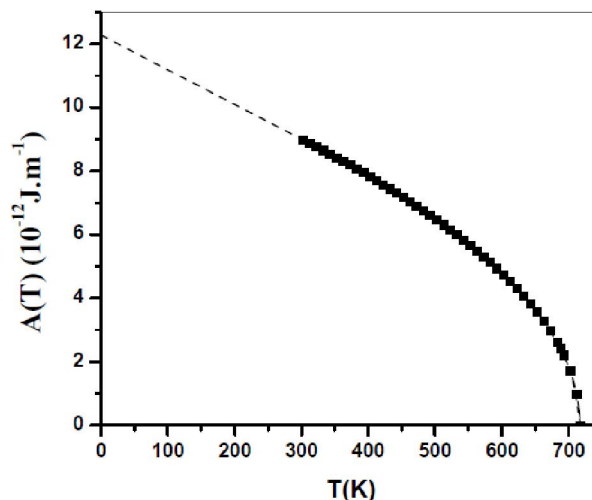


Figure 12 : The effect of temperature on the exchange constant for $CuFe_2O_4$

(hump shape) superimposed upon a general rise, as the Curie point is approached. While the other samples of $x = 0.2 - 0.3$, show a monotonic stabilization of μ_i with temperature and this behaviour is similar to the behaviour of a single domain^[23]. The secondary permeability maximum (SPM) is occur due to the anisotropy constant K_1 ^[24], which varies with temperature tending to zero at the transition temperature T_C .

It is known that the initial permeability μ_i is believed to arise as the result of reversible displacements of magnetic domain walls within the material. Rotation of spins within a domain, referred to as domain rotations, contribute little, on account of the relatively high magnetocrystalline anisotropy^[18]. Figure 11 shows the relation between μ_i and porosity. It is observed that the initial permeability decreases with increasing porosity. This behaviour may be related to samples whose porosity is too great (i.e. contain many pores) which hinder the movement of the domain wall causing the decrease in μ_i . Also, the effect of grain diameter on the magnitude of the initial permeability is shown in TABLE 1. It is observed that the initial permeability increases with further increasing in grain diameter for $D \geq 15 \mu m$. This behaviour may be attributed to below 15 microns; the decrement in μ_i may be related to the pores that occur in the crystals, and these, limit the permeability. Then for larger grains, the permeability increases due to domain wall displacements.

The magnitude of the initial permeability of a magnetic material as a result of rotations is proportional to

the square of the saturation magnetization and inversely proportional to the magnetic anisotropy energy according to the relation^[25]:

$$\mu_i = \frac{M_s^2 \cdot D}{\sqrt{K_1}} \quad (4)$$

From this relation we calculate the value of the anisotropy constant K_1 for each composition.

Guyot and Globus^[26,27] have established a direct relation between the hysteresis losses and the domain wall energy. The domain wall energy is calculated according to the relation:

$$\sigma_w = 2\sqrt{AK_1} \quad (5)$$

where: A is the exchange constant, which is calculated from the relation^[26]:

$$A(T) = \frac{k_B T_C}{a} \left(1 - \frac{T}{T_C} \right)^{1/2} \quad (6)$$

The term (kb) is known the exchange energy stored in the transition layer resulting from the spin interaction^[24], and a is the lattice constant. The Right H.S. vs. T is represented in figure 12 for $x = 0.0$ as a representative example. The extrapolated experimental value of the thermal variations of A(T) i.e. the values of A(0) are given in TABLE 1 and very coincident with the calculated values.

If δ_w is thickness of the domain wall, the total wall energy per cm^2 is given by:

$$\sigma_w = K_1 \delta_w \quad (7)$$

Form the two relations (5&6), δ_w was calculated and tabulated in TABLE 1 for each composition. It is found that all the obtained results are in good agreement with the values in the literature^[17,24].

CONCLUSION

The decrease in magnetization and Curie temperature with the addition of Ge content is suggested to be due to the decrease in A-B interaction according to Néel's molecular field theory.

The two parameters coercive field H_C and the relative magnetization m_r decrease with increasing temperature. This behaviour is explained through Brown's relation.

The thermal analysis of μ_i show a secondary peak

(hump shape) below T_C for $x=0.0$ up to 0.15. While the other samples of $x=0.2, 0.25$ and 0.3 show a monotonic stabilization behaviour of μ_i with T.

The domain wall energy and domain wall thickness were in the order of 10^{-3} J/m^3 & 10^{-8} m , respectively and were dependent on Ge concentration.

REFERENCES

- [1] H.Mocuta, L.Lechevallier, J.M.Le Breton, J.F.Wang, I.R.Harris; *J.Alloys and Compds.*, **364**, 48-52 (2004).
- [2] S.Manjura Hoque, Md.Amanullah Choudhury, Md.Fakhrul Islam; *J.Mag.and Mag.Mat.*, **251**, 292-303 (2002).
- [3] D.Ravinder, P.Vijaya Bhasker Reddy; *Mat.Lett.*, **57**, 1732-1737 (2003).
- [4] S.A.Mazen, M.H.Abdallah, M.A.Elghandoor, H.A.Hassen; **144**, 461-470 (1994).
- [5] S.A.Mazen, A.Eljalaky, H.A.Hashem; *Appl.Phys. A*, **61**, 559 (1995).
- [6] D.S.Birajdar, U.N.Devatwal, K.M.Jadav; *J.Mat. Sci.*, **37**, 1443-1448 (2002).
- [7] Misbah Ul-Islam, Tahir Abbas, M.Ashraf Chaudhry; *Mat.Lett.*, **53**, 30-34 (2002).
- [8] M.Manjurul Haque, M.Huq, M.A.Hakim; *J.Mag. and Mag.Mat.*, **320**, 2792-2799 (2008).
- [9] Jimin Du, Zhimin Liu, Weize Wu, Zhonghao Li, Buxing Han, Ying Huang; *Mat.Res.Bull.*, **40**, 928-935 (2005).
- [10] S.A.Mazen; *Mat.Chem.and Phy.*, **62**, 131-138 (2000).
- [11] S.A.Mazen, H.M.Zaki; *Phys.Stat.Sol.(a)*, **199**, 305-320 (2003).
- [12] S.A.Mazen, M.H.Abdallah, B.A.Sabrah, H.A.Hashem; *Phys.Stat.Sol.(a)*, **134**, 263-271 (1992).
- [13] A.D.Al-Rawas, A.Rais, A.A.Yousif, A.M.Gismelseed, M.E.Elzain, S.Mazen, A.Al-Falaky; *J.Mag.and Mag.Mat.*, **269**, 168-175 (2004).
- [14] S.A.Mazen, N.I.Abu-Elsaad; *J.Mag.and Mag.Mat.*, **322**, 265 (2010).
- [15] S.A.Mazen, S.F.Mansour, E.Dhahri, T.A.Elmosalami, H.M.Zaki; *Mat.Chem.and Phy.*, **117**, 51-58 (2009).
- [16] S.A.Mazen, A.H.Wafik, S.F.Mansour; *J.Mat.Sci.*, **31**, 2661-2665 (1996).
- [17] J.Smit, H.P.J.Wijn; *Les Ferrites 'Ferrites'*, Philips Technical Library, Dunod, Paris, (1961).

Full Paper

- [18] K.J.Standley; 'Oxide Magnetic Materials', Charendon Press, Oxford, (1972).
- [19] B.J.Evans, S.S.Hafner; J.Phys.Chem.Sol., **29**, 1573-1588 (1968).
- [20] S.A.Mazen, A.A.Yousif, M.E.Elzain; Phys.Stat. Sol.(a), **149**, 685-690 (1995).
- [21] J.M.D.Coey; 'Rare-earth Permanent Magnetism', Published by John Wiley and Sons, New York, (1996).
- [22] S.Chikazumi, S.Charap; 'Physics of Magnetism', Published by John Wiley and Sons, Inc., New York, (1964).
- [23] S.Unnikrishnan, D.K.Chakrabarty; Phys.Stat. Sol.(a), **121**, 265-271 (1990).
- [24] Alex Goldman; 'Modern Ferrite Technology', Marcel Dekker, New York, (1993).
- [25] G.C.Jain, B.K.Das, R.S.Khanduja, S.C.Gupta; J.Mat.Sci., **11**, 1335-1338 (1976).
- [26] M.Guyot, A.Globus; J.de Phys.Colloques, **38**, C1-157 (1977).
- [27] M.Guyot, A.Globus; Phys.Stat.Sol.(b), **59**, 447-454 (1973).